

## Article

# Design, Synthesis and Antibacterial Studies of Novel Cationic Amphipathic Cyclic Undecapeptides and Their Linear Counterparts against Virulent Bacterial Strains

Hisham N. Farrag, Toshinari Maeda and Tamaki Kato \*

Department of Biological Functions Engineering, Graduate School of Life Science and Systems Engineering, Kyushu Institute of Technology, Wakamatsu Campus, Fukuoka Prefecture, Kitakyushu City 808-0196, Japan; farrag.hisham320@mail.kyutech.jp (H.N.F.); toshi.maeda@life.kyutech.ac.jp (T.M.)

\* Correspondence: tmkato@life.kyutech.ac.jp

**Abstract:** Bacteria have acquired resistance against almost all antibiotics because of the misuse of antibacterial agents and long periods of treatment. Antimicrobial peptides (AMPs) are one of the most encouraging candidates to solve this problem, as they possess high prokaryotic selectivity, and affect the bacteria by a unique mode of action. Novel cyclic undecapeptides (QNRNFYFNRNQ and QNRNFHFNRNQ) and their linear counterparts were investigated for their antibacterial activity against virulent strains. The minimal inhibitory concentration (MIC) values showed that tyrosine and histidine AMPs have promising antibacterial activity against virulent bacteria. The MIC values against the *P. aeruginosa* PA14, *E. coli* O157:H7 CR3, *S. aureus* 209P, and *B. subtilis* ATCC 6633 bacterial strains were evaluated for the cyclic peptide containing tyrosine, and their values were 6.25, 12.5, 12.5, and 12.5  $\mu\text{M}$ , respectively. Meanwhile, for the linear form, they were 9.3, 12.5, 12.5, and 12.5  $\mu\text{M}$ , respectively. The cyclic-peptide-containing histidines' MIC values were 6.25, 3.1, 6.25, and 3.1  $\mu\text{M}$ , respectively. Meanwhile, for the linear form, they were 3.1, 3.1, 3.1, and 6.25  $\mu\text{M}$ , respectively. The antibacterial activities of the new AMPs were compared with that of gentamicin sulfate, and showed relatively higher potencies. Time-inhibition studies demonstrated the rapid antibacterial effects of the novel AMPs, which were more likely to be concentration-dependent, rather than time-dependent. At double the MIC concentration, all of the tested peptides exhibited relatively stable antibacterial effects up to 24 h, especially the peptides containing tyrosine, which showed an improved antibacterial effect.

**Keywords:** antibiotics; AMPs; cyclic undecapeptides; virulent bacterial strains; gentamicin



**Citation:** Farrag, H.N.; Maeda, T.; Kato, T. Design, Synthesis and Antibacterial Studies of Novel Cationic Amphipathic Cyclic Undecapeptides and Their Linear Counterparts against Virulent Bacterial Strains. *Sci. Pharm.* **2021**, *89*, 10. <https://doi.org/10.3390/scipharm89010010>

Received: 2 December 2020

Accepted: 26 January 2021

Published: 5 February 2021

**Publisher's Note:** MDPI stays neutral with regard to jurisdictional claims in published maps and institutional affiliations.



**Copyright:** © 2021 by the authors. Licensee MDPI, Basel, Switzerland. This article is an open access article distributed under the terms and conditions of the Creative Commons Attribution (CC BY) license (<https://creativecommons.org/licenses/by/4.0/>).

## 1. Introduction

The prevalence of nosocomial-acquired and community-developed diseases due to many virulent bacterial strains, such as *Pseudomonas aeruginosa*, *Staphylococcus aureus*, *Escherichia coli*, and *Bacillus subtilis*, have been growing recently [1]. The global emergent catastrophe of antibiotic resistance acquired by the virulent bacterial strains has underlined the necessity of the investigation of new substitutes for currently-existing antibiotics [2]. Antimicrobial peptides (AMPs) have arisen as a substitutive therapy for the treatment of antibiotic-resistant pathogens, as they can eradicate bacteria and enhance the body's defenses at the same time [3,4]. Cationic AMPs uniquely affect microbes by targeting the negatively-charged membrane lipids, which can decrease the incidence of microbial resistance [5]. AMPs are short peptides containing a few amino acid residues, organized in variable sequences.

AMPs kill microorganisms by several mechanisms of action [6,7], but generally, there are two predominant mechanisms. The first is by attacking the bacterial cell membranes. The amphipathic moieties included in AMPs initiate the interaction with the bacterial cell membranes. The amphipathic character of a peptide indicates the presence of hydrophobic

and cationic residues incorporated in the sequence. These moieties start the interaction between the peptides and bacterial cell membranes through hydrophobic and electrostatic forces. These forces allow the peptide to penetrate the bacterial cell membranes, causing cell death [8]. The other mechanism of AMPs is the targeting of some vital cell components, such as DNA [9].

The charge of the bacterial cell membrane is an important factor determining the biological efficacy of AMPs. Bacteria show no growth when they are attached to positively-charged surfaces, which explains the importance of the cationic residues incorporated in the peptide [10]. The hydrophobic moieties facilitate the diffusion of AMPs inside the bacterial cell membrane by hydrophobic interactions. Additionally, hydrophobic residues initiate the formation of the secondary structures via a self-assembly process in the bacterial cell membrane [11]. Some AMPs are self-assembled into  $\alpha$ -helical shapes with the hydrophilic side chains organized along one side, while the hydrophobic side chains are arranged on the other side. Other AMPs are arranged into  $\beta$ -sheet structures. These secondary structures represent the active forms of the peptides which facilitate the interaction with bacterial cell membranes.

Herein, new cationic amphipathic cyclic undecapeptides and their linear counterparts were studied for their antibacterial behavior against the virulent bacterial strains *Escherichia coli* (*E. coli*), *Pseudomonas aeruginosa* (*P. aeruginosa*), *Bacillus subtilis* (*B. subtilis*), and *Staphylococcus aureus* (*S. aureus*). These peptides were designed to have symmetric amino acid sequences with a distinguishing residue in the center. The first peptide (1) is a linear undecapeptide with the following amino acid sequence: H-QNRNFYFNRNQ-OH (all amino acids are in the L-configuration), and (2) is its cyclic form. Eight cationic and polar moieties were added in order to encourage the interaction with the negatively charged bacterial cell wall, and to increase the peptide solubility. The hydrophobicity of the compound depends on two phenylalanine residues to initiate the interaction with the bacterial cell membrane lipids. Tyrosine was incorporated into the peptide center for its amphipathic behavior. Another analog was designed by replacing the tyrosine with histidine, ((3) and (4)), in order to study the effect of this change on the antibacterial activity of the tested peptides. The symmetric wings QNRNF (Y or H) FNRNQ were designed to optimize the interaction with the bacterial cell wall. Most previous studies utilized cationic residues for the electrostatic interactions, but here we used six polar residues and two cationic residues in order to reduce or eliminate the harmful effect on human cells [12]. Arginine (R) is a cationic residue for the electrostatic interaction with the bacterial cell wall's negatively charged components. Arginine was supported with two polar asparagine (N) residues for weak electrostatic interaction (hydrogen bonding). The cell-penetrating residues are the hydrophobic residues. Our main goal was to study the difference in the penetration ability of both analogs. We postulated that the presence of tyrosine residue in the center of two phenylalanine residues would create a highly-penetrating nucleus. This nucleus, Phe-Tyr-Phe, can penetrate the bacterial cell membrane through hydrophobic interactions. The amphipathic character of tyrosine augmented these interactions and improved the penetration of the peptide into the bacterial cell membranes [8].

To date, the structural activity relationship (SAR) for AMPs is still at a growing stage, which requires further extensive studies. Figure 1 illustrates the suggested mechanism of action of the novel AMPs. First, they attach themselves to the lipopolysaccharide layer in Gram-negative bacteria, and the lipoteichoic acid moieties in the peptidoglycan layer of Gram-positive bacteria. Cationic residues initiate electrostatic interaction forces towards the negatively-charged bacterial cell membrane components. The amphipathic structure of the novel peptides gives them the ability to create secondary structures inside the bacterial cell wall [8]. The hydrophobic moieties facilitate the penetration of the peptides into the bacterial cells by diffusion through the lipid bilayers, leaving holes across the cell membranes, causing membrane degeneration and the death of the bacterial cells [13].

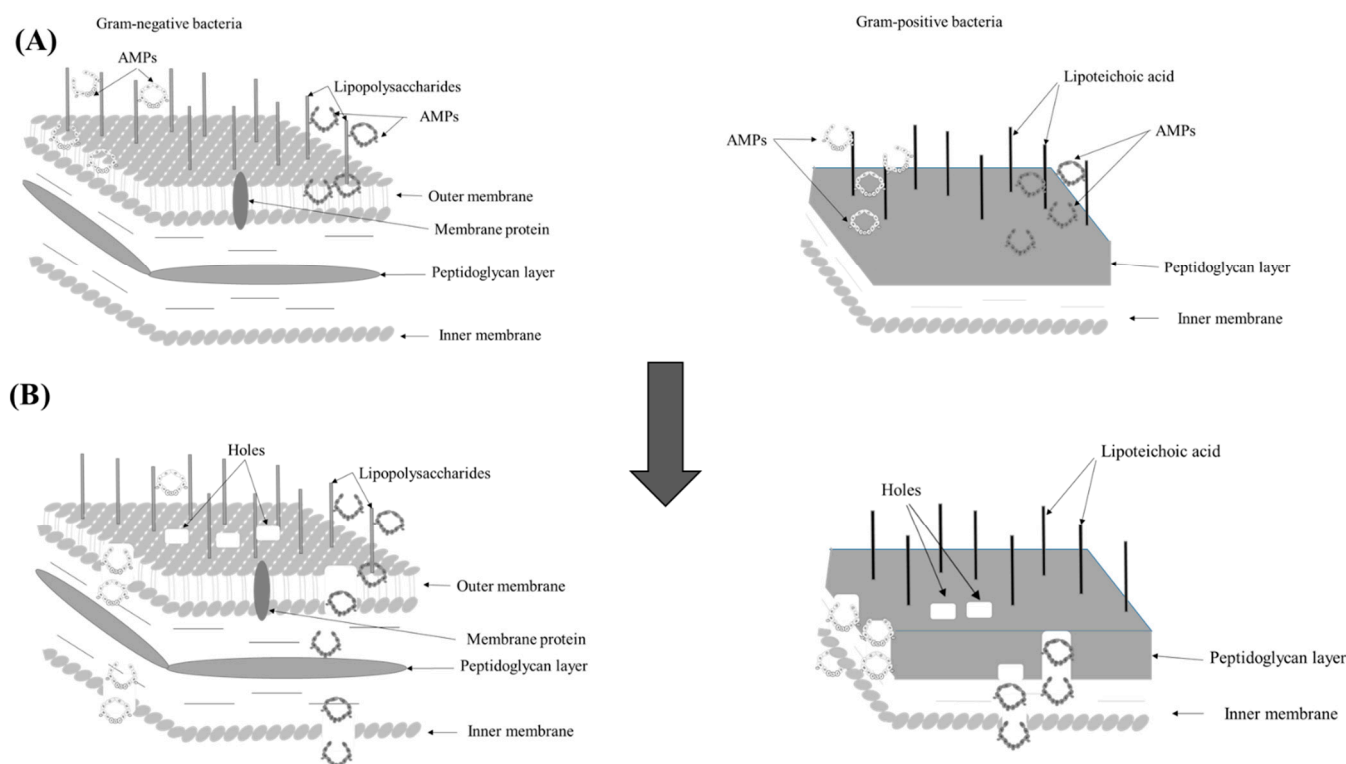


**Figure 1.** The suggested mechanism of action of the novel AMPs. (A) The electrostatic interactions between the peptides and negatively-charged bacterial cell walls. (B) The penetration of the peptides into the bacterial cell walls, leaving holes behind.

## 2. Materials and Methods

### 2.1. Materials

The theoretical molecular weights of (1), (3), (4), and (2) were calculated as 1501, 1475, 1457, and 1482, respectively, using ChemDraw 16.0 software. The linear peptides were prepared via a standard Solid-Phase Peptide Synthesis method using 9-fluorenylmethoxycarbonyl (Fmoc) chemistry and 2-chlorotrityl resin as the solid support [14]. All of the Fmoc-protected amino acids, resin, piperidine, O-benzotriazole-*N,N,N',N'*-tetramethyluronium hexafluorophosphate (HBTU), 1-hydroxybenzotriazole hydrate (HOBt·H<sub>2</sub>O), *N,N*-diisopropylethylamine (DIPEA), and 2,2,2-trifluoroacetic acid (TFA) were purchased from Watanabe Chemical Industries, Ltd., Hiroshima, Japan. The other reagents and solvents were purchased from Wako Pure Chemical Industries, Ltd., Osaka, Japan.

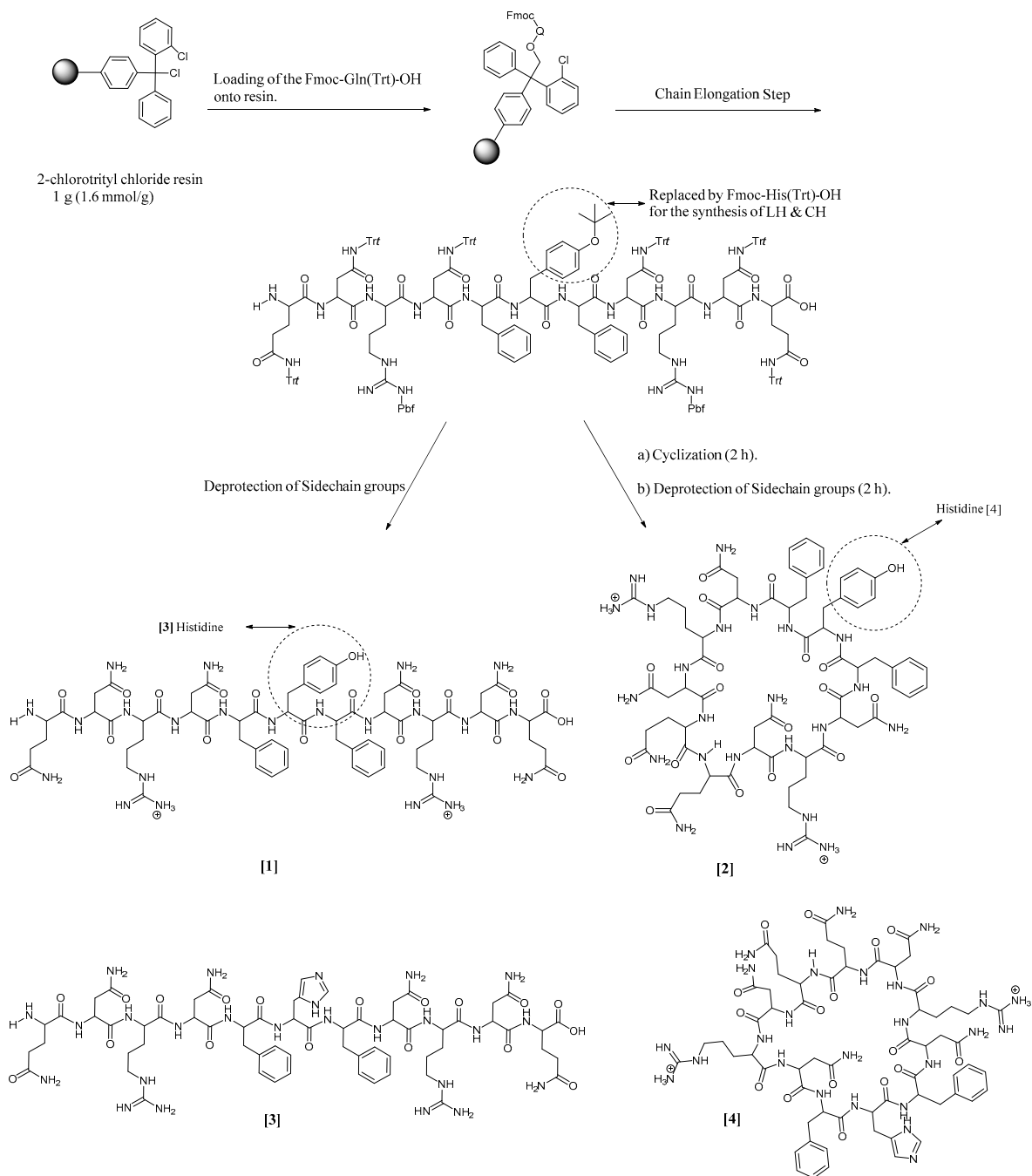
### 2.2. Synthetic Protocol

The standard Fmoc solid-phase peptide synthesis method was used to synthesize all of the four peptides—(4), (3), (2), and (1)—as depicted in Scheme 1. The synthetic process was started by loading a protected glutamine amino acid (1 mmol) onto 1 g 2-chlorotrityl chloride resin (1.6 mmol/g) using 1.5 equivalents DIPEA in 30 mL dichloromethane (rotated for 1 h). The unreacted sites on the resin were capped by adding 1 mL methanol to the reaction mixture (rotated for 10 min). Sidechain protected Fmoc-L-amino acid residues (2 Equivalents) were then coupled to the loaded glutamine residue using 2 equivalents of HBTU (2 mmol), 4 equivalents of DIPEA (0.7 mL) and 2 equivalents of HOBt in 30 mL *N,N*-dimethylformamide (DMF) as a solvent for the coupling process. The coupling process was carried out for two hours at room temperature. In total, 20% (*v/v*) piperidine in DMF (30 mL) was used to remove the Fmoc-protecting groups, which was accomplished in 30 min at room temperature. The cleavage of the sidechain-protected linear undecapeptide from the resin was achieved using a mixture of 2,2,2-trifluoroethanol (TFE) (18 mL)/acetic acid (6 mL)/dichloromethane (DCM) (6 mL) in a ratio of 3:1:1 (*v/v/v*) [15]. The removal of the

sidechain-protecting group was carried out for two hours at room temperature. Purification was carried out by using a semi-preparative RP-HPLC Hitachi L-7100 apparatus fortified with an XTerra Prep MS C18 OBD 10  $\mu\text{m}$  column (19  $\times$  150 mm; Waters). The mobile phases were acetonitrile containing 0.1% TFA (solvent B), and H<sub>2</sub>O containing 0.1% TFA (solvent A). The elution gradient was 0–100% of solvent B. The flow rate was adjusted to 5 mL/min at room temperature. The peak intensity was determined at a wavelength of 220 nm [16]. The removal of the sidechain-protecting groups was achieved using a mixture of TFA/trisopropylsilane (TIS)/H<sub>2</sub>O at a ratio of 95:2.5:2.5 (v/v/v). The lyophilization was carried out in a VD-800F freeze dryer (TAITEC). The cyclization reaction was achieved by the use of a low concentration of 0.5 mM from (1) to avoid dimer formation. HBTU (2 equivalents) and DIPEA (5 equivalents) were used for the cyclization process. The removal of the sidechain-protecting groups of (2) was carried out using a mixture of TFA/TIS/H<sub>2</sub>O at a ratio of 95:2.5:2.5 (v/v/v) at room temperature. Purification was achieved by a semi-preparative RP-HPLC, followed by lyophilization to yield the targeted pure final cyclic product [17]. (3) and (4) have been synthesized by the same method; the only difference is in the central amino acid residue (replacing the tyrosine residue with a histidine residue). The synthetic process was elucidated by HPLC, as shown in Figures S1–S4.

### 2.3. MIC Evaluation

The MIC values were determined by the broth micro-dilution method using 96-well microplates with clear bottoms (Nunclon™ Surface, Roskilde, Denmark) [18]. *P. aeruginosa* PA14, *S. aureus* 209P, *E. coli* O157:H7 CR3, and *B. subtilis* ATCC 6633 were chosen as tester bacterial strains to determine the broad-spectrum effect of the new undecapeptides (1), (2), (3), and (4) against Gram-positive and Gram-negative virulent bacterial strains. The bacterial strains were inoculated separately in a freshly prepared Luria Bertani (LB) broth medium at a temperature of 37 °C, and were then shaken at 120 rpm overnight. The cultures were diluted up to  $5 \times 10^5$  CFU/mL ( $\text{OD}_{600} = 0.05$ ). The peptide solutions were prepared by dissolving each type separately in dimethyl sulfoxide (DMSO), and were further diluted with water to reach a concentration of 1 mM. The percentage of DMSO was not more than 5% of the total volume. The peptide solutions (0.1 mL) were added to 0.9 mL of the broth media to a starting concentration of 100  $\mu\text{M}$ . Serial 2-fold dilutions were applied to reach a concentration of 0.09  $\mu\text{M}$ , distributed across the 96-well microplates. The positive controls were applied by using an aqueous solution of gentamicin sulfate as a broad-spectrum antibiotic, prepared at a concentration of 50  $\mu\text{M}$ , and diluted across the 96-well microplates by 2-fold serial dilutions. Runs without the antimicrobials were carried out in order to ensure the adequate growth of the bacteria. The bacterial cultures were mixed well with the tested compounds in a ratio of 1:39 (v/v). The  $\text{OD}_{600}$  values were determined using a Microplate reader (Varioscan Flash dispenser option—Thermo Scientific, Tokyo, Japan) which was used as a blank, because the tested compounds are partially insoluble in the media. The 96-well microplates were incubated for 24 h at 37 °C, and the  $\text{OD}_{600}$  values were determined again after 24 h. The MIC values were determined as the minimal concentration where no visible bacterial growth was detected, and were confirmed by subtracting the  $\text{OD}_{600}$  values at 0 h (before the incubation) from the  $\text{OD}_{600}$  values at 24 h. All of the experiments were carried out in biological duplicates.



**Scheme 1.** The synthetic protocol of the novel undecapeptides (1), (2), (3), and (4) by a standard Fmoc solid-phase peptide synthesis method, followed by peptide cyclization using a standard liquid-phase system.

#### 2.4. Time-Inhibition Studies

Time-inhibition assays were conducted against the *P. aeruginosa* PA14, *S. aureus* 209P, *E. coli* O157:H7 CR3, and *B. subtilis* ATCC 6633 bacterial strains. Clear-bottomed 96-well microplates (Nunclon™ Surface, Roskilde, Denmark) were used for the assays. The bacterial cultures were prepared as previously mentioned. The antibacterial effects were evaluated by measuring the OD<sub>600</sub> values at different time intervals using a Microplate reader (Varioscan Flash dispenser option—Thermo Scientific) and compared with the OD<sub>600</sub> values determined before the addition of the bacterial cultures (blank values). The peptides (LH, CH, LY, and CY) were tested at concentrations of double the MIC values. Runs without the antimicrobials were performed in order to confirm the adequate growth

of the bacteria. The bacterial cultures were mixed with the tested peptides and incubated at 37 °C for 24 h. The OD<sub>600</sub> values were measured at different time intervals—0, 4, 8, 18, and 24 h—to determine the survival of the bacterial cells. The bacterial growth (viability) percentages were calculated according to the following equation: %viability = (OD<sub>600</sub> value of the tested antibiotic/OD<sub>600</sub> value of the negative control) × 100. Consequently, the %inhibition were calculated using the following equation: %inhibition = 100 – % growth (%viability). The inhibitory effects of the tested peptides were calculated before the incubation (0 h), and were compared with the negative controls, which consisted of the media, solvents, and bacteria. These controls' OD<sub>600</sub> values (control for each bacteria) were estimated at the same time intervals as the tested peptides, and were compared with them at each specific time. The time-inhibition assays were conducted in duplicates.

### 3. Results and Discussion

#### 3.1. Design of Peptides

QNRNF (Y or H) FNRNQ was designed to possess two cationic residues and six polar residues in order to assist in the electrostatic interactions with the bacterial cell wall. The hydrophobic moieties are two phenylalanine for the penetration into the cell. Tyrosine has an amphipathic character to assist in the penetration. Histidine was selected to replace tyrosine for its cationic properties, which can affect the antimicrobial effect. The cyclized form provides a rigid and more stable structure than its linear counterpart, which increases the antibacterial effect. The global minimum conformations of 3D ribbon-structures were computationally obtained using the LowModeMD, and the minimization energies were –543.8, –561.3, –436.5, and –440.6 kcal/mol for (3), (1), (4), and (2), respectively. The Low Mode Search enables the exploration of low-energy conformation, which takes into account the complex non-bonded interactions [19].

#### 3.2. Synthesis and Characterization

For comparative studies, peptides (1) and (2) were designed to possess positively-charged, polar, amphipathic (tyrosine residue), and hydrophobic moieties. Meanwhile, peptides (4) and (3) were designed to have polar, hydrophobic, and more positively-charged (the added histidine residue) moieties. The predicted structures of the newly synthesized AMPs in 3D conformations can be seen in Figure 2. The % yield of the obtained peptide (1) was about 98%, while that of (2) was about 75%. The structure and purity of all of the synthesized peptides were confirmed by MALDI-TOF Mass Spectrometry, and the molecular weights that were found for (1), (3), (4), and (2) were 1501 [M]<sup>+</sup>, 1475 [M]<sup>+</sup>, 1459 [M+2H]<sup>+</sup>, and 1482 [M]<sup>+</sup>, respectively, as depicted in Figures S5–S8. The purity reached more than 99% after purification with a semi-preparative RP-HPLC. Similarly, 99% peptides (3) and (4) were obtained after purification using a preparative RP-HPLC, and their %yields were about 97% and 75%, respectively.

#### 3.3. MIC Evaluations

The MIC values against the *P. aeruginosa* PA14, *S. aureus* 209P, *E. coli* O157:H7 CR3, and *B. subtilis* ATCC 6633 bacterial strains were evaluated for all of the peptides, as shown in Table 1. Generally, all of the peptides showed high activities with low MIC values against all bacterial strains. The histidine peptides displayed relatively higher potencies against all of the bacterial strains, with MIC values ranging from 3.1 to 6.25 µM. Meanwhile, (1) and (2) showed slightly lower potencies, with MIC values ranging from 6.25 to 12.5 µM. The linear histidine peptide (3) displayed an enhanced antibacterial effect in comparison to that of the cyclic peptide (4). In the case of *P. aeruginosa* and *S. aureus*, (3) was more potent, whereas (4) showed more antibacterial activity against *B. subtilis*, while both of them displayed the same antibacterial effect against *E. coli*. Gentamicin sulfate [GS] was used as a standard control for all of the bacterial strains in order to ensure the validity of the experiment, and also to compare its effect with the tested peptides. Against the *P. aeruginosa* and *S. aureus* bacterial strains, (3) was the most effective antibacterial agent,

compared with other peptides and gentamicin sulfate. Meanwhile, (3), (4), and GS had the same effect against *E. coli*, whereas GS was the most effective antibacterial agent against the *B. subtilis* bacterial strain.

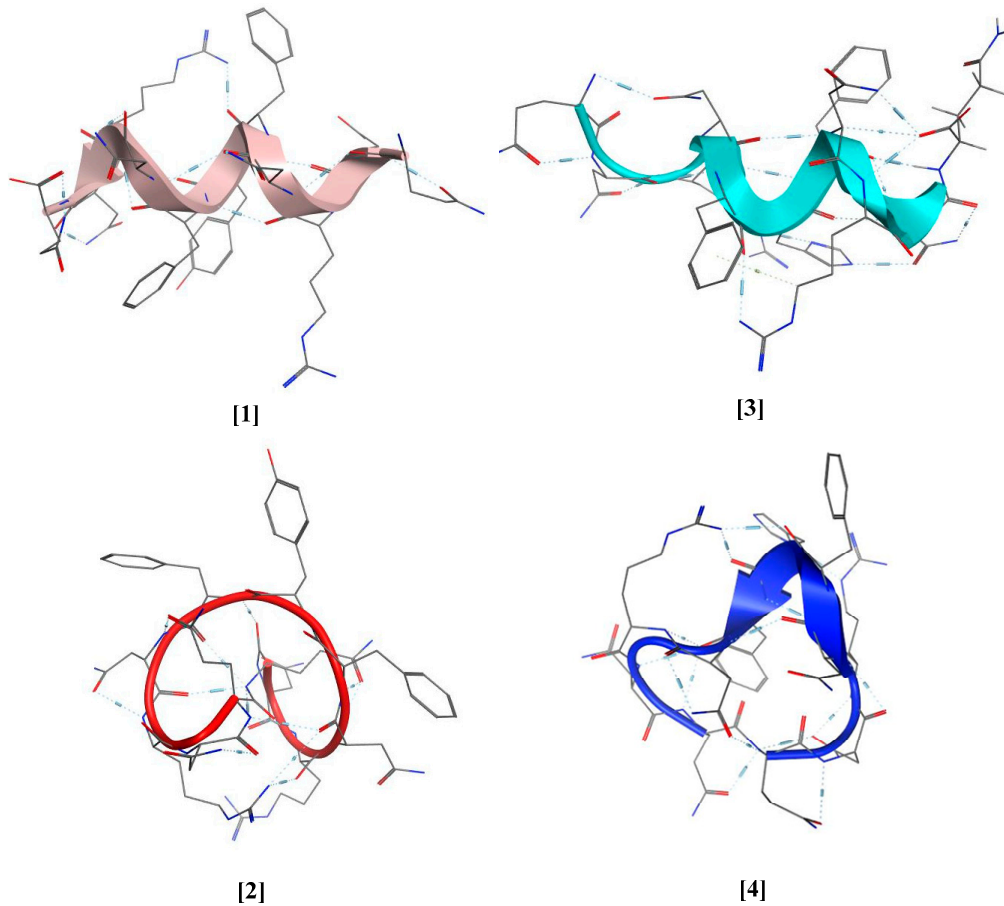


**Figure 2.** The 3D global minimum conformation of the ribbon-structures of the newly synthesized AMPs computationally predicted using MOE 18.0.

**Table 1.** MIC values of the novel undecapeptides against Gram-negative and Gram-positive strains.

Peptide	MIC Values ( $\mu\text{M}$ )			
	<i>P. aeruginosa</i>	<i>E. coli</i>	<i>S. aureus</i>	<i>B. subtilis</i>
(1)	9.3	12.5	12.5	12.5
(2)	6.25	12.5	12.5	12.5
(3)	3.1	3.1	3.1	6.25
(4)	6.25	3.1	6.25	3.1
Gentamicin sulfate [GS]	6.25	3.1	6.25	1.6

### 3.4. Time Inhibition Assays

Figure 3A showed the antibacterial behavior of the novel AMPs against *S. aureus* at five different time intervals. All of the tested AMPs had good and stable antibacterial effects against *S. aureus*. During the 24 h of incubation, (3) had a relatively higher efficacy, as it could reach more than 99.99% inhibition from the beginning of the test. Furthermore, (2) and (1) showed high efficacies during the test period, with more stable antibacterial effects. Lastly, (4) showed a relatively lower effect compared to (3), (1), and (2). As described in Figure 3B, (2) showed the maximum antibacterial effect against *P. aeruginosa* PA14 at double the MIC value. Additionally, its antibacterial activity was unwavering over the

whole period of incubation, as it affects more than 99.99% of the bacteria from the beginning of the incubation. In terms of efficiency, (1) come next to (2), showing a remarkable antibacterial effect, as it affected more than 97% of the bacteria from the start of the reaction. In comparison with (1) and (2), (4) and (3) exhibited slightly lower efficacies, as they started by inhibiting more than 95% and 92% of the bacterial growth, respectively, while their full effect was only exerted after 24 h of incubation. As illustrated in Figure 3C, (2) and (1) had the most active and stable antibacterial pattern. They could affect more than 97% of the bacteria at 0 h of incubation. Furthermore, (2) was more effective against *E. coli* than (1) and other peptides. However, (3) and (4) showed the maximum antibacterial effect at 24 h of incubation, and the bacteria showed little resistance against them. As shown in Figure 3D, (2) was the most potent AMP against *B. subtilis*, with a stable antibacterial effect over the examination time, except after 4 h. However, after 8 h, the peptide could overcome the bacterial resistance, reaching more than 99.99% inhibition of the bacterial growth. Additionally, (1) was the second peptide in efficacy, as it could overcome the bacterial resistance after 4 h of incubation. However, the bacteria could resist the antibacterial effect of (4) and (3) from 4 h until 18 h. After that, they could inhibit more than 95% and 99.99% of the bacteria, respectively.

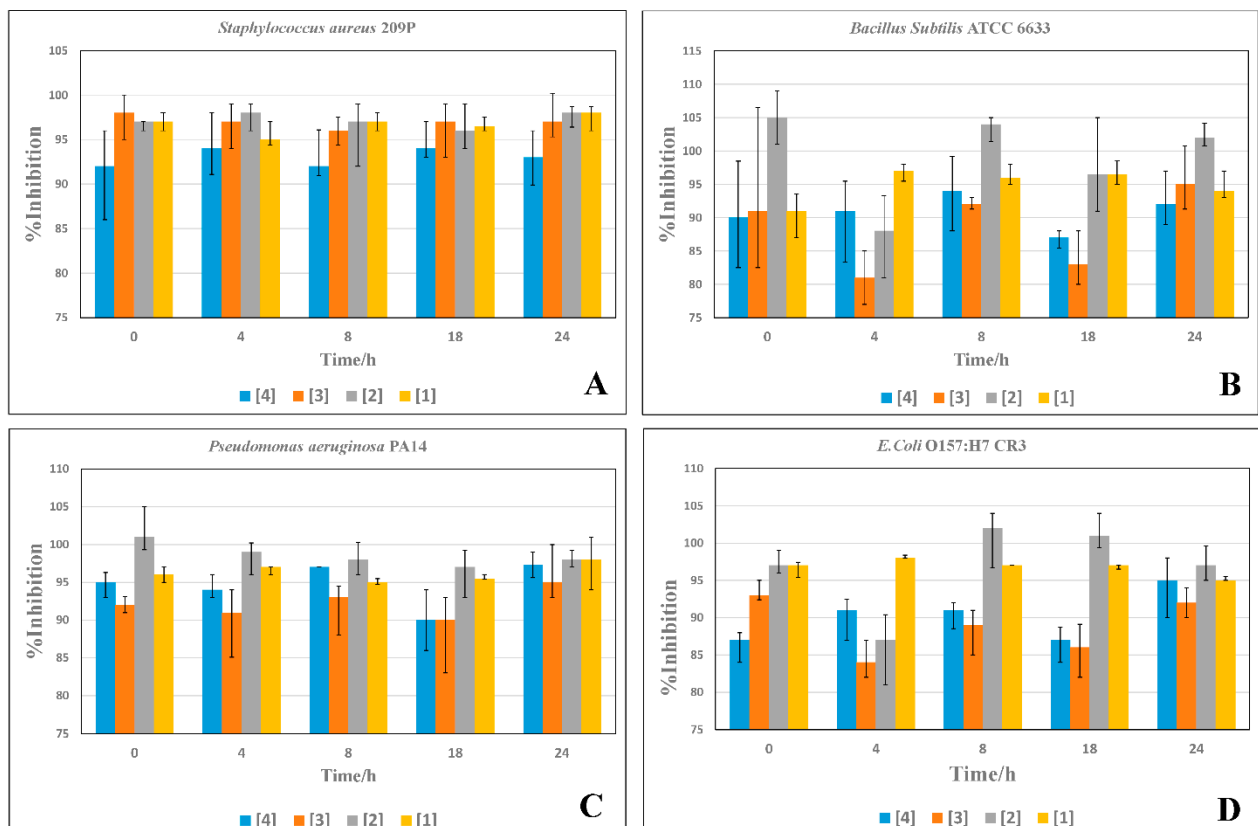
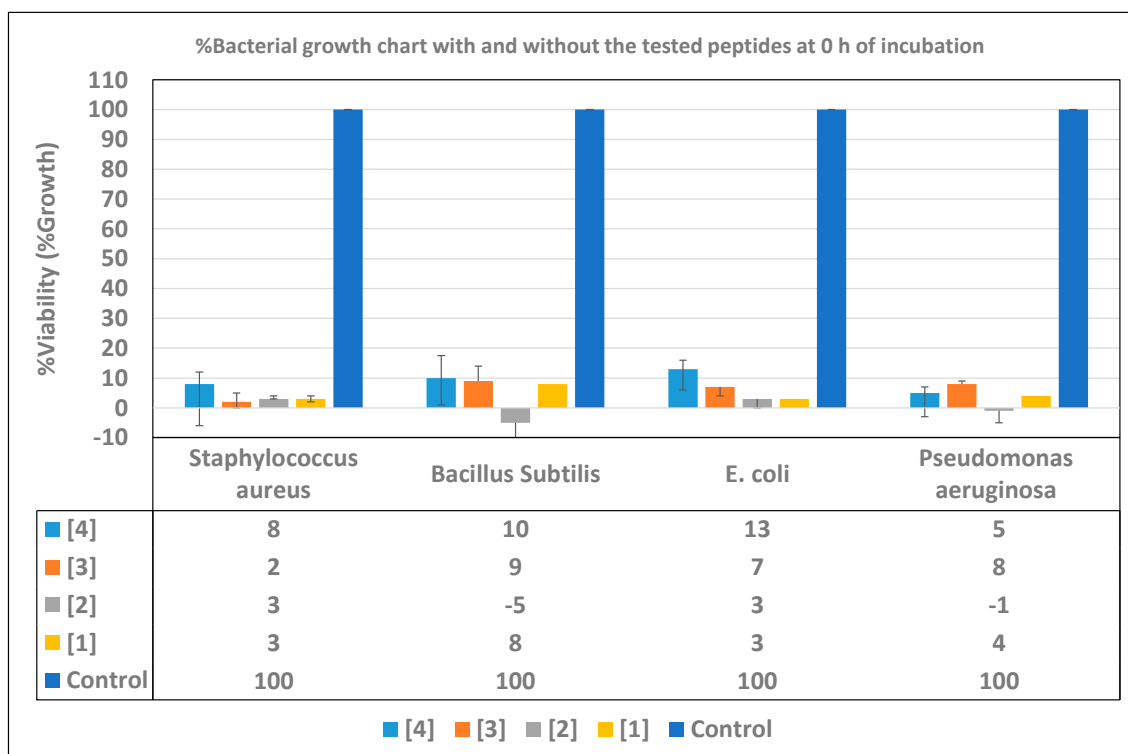


Figure 3. Time-inhibition assays of the newly-synthesized AMPs against the selected bacterial strains (A–D).

The results described in Figure 4 show the inhibition of the bacterial growth in the tested samples compared with the controls before incubation. We can see that (2) showed relatively high activity (except for *S. aureus*), as it could inhibit the growth of *P. aeruginosa* and *B. subtilis* completely, while the %growth of the other bacteria was about 3%. According to the activity, (1) came in second place, except for against *S. aureus*, for which it showed the same efficacy as (2). In addition, (3) came in third place according to its activity against all bacteria except for *S. aureus*; it was the most active peptide, as its associated bacterial growth was about 2%. While (4) showed a good antibacterial activity, it was relatively lower than the other peptides except for *P. aeruginosa*; it was more active than (3).



**Figure 4.** The growth percentage chart of the bacteria in the presence of the newly-synthesized AMPs, compared with the negative controls before the incubation (at 0 h of incubation).

The antibacterial property of the cyclic peptide (2) fares better compared with (1). This higher activity depends on the more rigid structure and the higher hydrophobicity of the cyclic conformation, allowing (2) to penetrate the bacterial cell more effectively than the linear peptide, causing a more inhibitory effect on the bacterial growth. Replacing the tyrosine residue with a histidine slightly improved the overall antibacterial effect of (3) and (4) over that of the (1) and (2) peptides. We suggest that the increase in the antibacterial effect is due to the positively-charged histidine residue located in the center of the two phenylalanine residues, which creates a relatively stronger attacking nucleus. This nucleus has more penetrating ability into the bacterial cell membrane than that of the tyrosine nucleus. Besides this, the secondary structure created by (3) can penetrate the bacterial cell membranes more rapidly than its cyclic form.

The cell-penetrating abilities of (3) and (4) were slightly augmented by the electrostatic interaction of the positively-charged histidine residue with the negatively-charged bacterial membranes. We posited that this interaction occurred during the penetration of the hydrophobic sidechain groups surrounding the histidine moiety. These double interaction forces increase the penetration rate of the peptide, causing the higher inhibition of bacterial cell growth. In addition, the Phe-His-Phe nucleus showed a better antibacterial effect in the linear form than that of the cyclic peptide, except in the case of *B. subtilis* bacterial strain. We assume that this nucleus penetrates the bacterial cell membrane more efficiently when it is connected to a free linear structure rather than the cyclic rigid form (i.e., the secondary structure of the linear form was more active and flexible than that of the cyclic form). *B. subtilis* is one of the spore-forming bacterial strains in which the rigid cyclic structure showed more penetrating ability into these persister cells than the linear form. The time-inhibition assays suggested a concentration-dependent, rather than time-dependent, inhibition of the bacteria by the tested peptides.

#### 4. Conclusions

The newly-designed cyclic cationic amphipathic undecapeptides and their linear counterparts were synthesized using a standard Fmoc SPPS method, with high yields of 75% and 97%, respectively. All of the peptides showed excellent antibacterial activities against Gram-negative (*P. aeruginosa*, and *E. coli*) and Gram-Positive (*S. aureus*, and *B. subtilis*) bacterial strains. The histidine-containing peptides showed higher potencies against all of the bacterial strains at lower concentrations. This is due to the suggested higher capability of their secondary structure formation at lower concentrations (assisted by the histidine residue) than (1) and (2). These secondary structures are responsible for the penetration of the bacterial cell membrane. This phenomenon explains the lower MIC values of histidine peptides, ranging from 3.1 to 6.25  $\mu\text{M}$ . Meanwhile, (1) and (2) showed lower potencies with higher MIC values—ranging from 6.25 to 12.5  $\mu\text{M}$ —than the histidine peptides. The time-inhibition assays proved the rapid antibacterial effects of both (2) and (1), as they could affect  $\geq 97\%$  of the bacterial strain at 0 h of incubation. Additionally, the bacterial resistance was negligible after incubation for 24 h, whereas (4) and (3) showed their maximum antibacterial effects after 24 h of incubation. We suggest that, at concentration levels of double the MIC values, the secondary structures of (1) and (2) can penetrate the bacterial cell membrane with higher impacts than the histidine peptides.

**Supplementary Materials:** The following are available online at <https://www.mdpi.com/2218-0532/89/1/10/s1>, Figures S1–S4: The HPLC charts of the newly synthesized AMPs, Figures S5–S8: MALDI TOF mass spectra of the novel AMPs.

**Author Contributions:** Conceptualization, H.N.F. and T.K.; methodology, H.N.F.; software, H.N.F.; validation, H.N.F.; formal analysis, H.N.F. and T.K.; investigation, H.N.F.; resources, T.M. and T.K.; data curation, T.K.; writing—original draft preparation, H.N.F.; writing—review and editing, T.K.; visualization, H.N.F.; supervision, T.M. and T.K.; project administration, T.K. All authors have read and agreed to the published version of the manuscript.

**Funding:** This research received no external funding.

**Institutional Review Board Statement:** Not applicable.

**Informed Consent Statement:** Not applicable.

**Data Availability Statement:** Data is contained within the article and Supplementary Materials.

**Acknowledgments:** We would like to express our profound gratitude to Shigeori Takenaka, Department of Applied Chemistry, Kyushu Institute of Technology, for his kind guidance and permission to use the MALDI-TOF Mass Spectrometer in his laboratory.

**Conflicts of Interest:** The authors declare no conflict of interest.

#### Abbreviations

(1)	Linear tyrosine peptide
(2)	Cyclic tyrosine peptide
(3)	Linear histidine peptide
(4)	Cyclic histidine peptide
GS	Gentamicin sulfate
MW	Molecular weight
Fmoc	9-fluorenylmethoxycarbonyl
HBTU	O-benzotriazole-N,N,N',N'-tetramethyl-uronium-hexafluorophosphate
HOBt·H <sub>2</sub> O	1-hydroxy-benzotriazole hydrate
DIPEA	N,N-diisopropylethylamine
TFA	2,2,2-trifluoroacetic acid
TFE	2,2,2-trifluoroethanol
TIS	Trisisopropylsilane
RP-HPLC	Reversed-phase high-performance liquid chromatography
DMSO	Dimethyl sulfoxide

TOF	Time of flight
OD	Optical density
MOE	Molecular Operating Environment

## References

1. Vincent, J. Nosocomial infections in adult intensive-care units. *Lancet* **2003**, *361*, 2068–2077. [[CrossRef](#)]
2. World Health Organization. *Global Priority List of Antibiotic-Resistant Bacteria to Guide Research, Discovery, and Development of New Antibiotics*; WHO: Geneva, Switzerland, 2017.
3. Diamond, G.; Beckloff, N.; Weinberg, A.; Kisich, K. The Roles of Antimicrobial Peptides in Innate Host Defense. *Curr. Pharm. Des.* **2009**, *15*, 2377–2392. [[CrossRef](#)] [[PubMed](#)]
4. Farrag, H.N.; Metwally, K.; Ikeno, S.; Kato, T. Design and Synthesis of a New Amphipathic Cyclic Decapeptide with Rapid, Stable, and Continuous Antibacterial Effects. *Pertanika J. Sci. Technol.* **2020**, *28*, 183–196. [[CrossRef](#)]
5. Lohner, K. New strategies for novel antibiotics: Peptides targeting bacterial cell membranes. *Gen. Physiol. Biophys.* **2009**, *28*, 105–116. [[CrossRef](#)]
6. Dutta, S.R.; Gauri, S.S.; Ghosh, T.; Halder, S.K.; DasMohapatra, P.K.; Mondal, K.C.; Ghosh, A.K. Elucidation of structural and functional integration of a novel antimicrobial peptide from *Antheraea mylitta*. *Bioorg. Med. Chem. Lett.* **2017**, *27*, 1686–1692. [[CrossRef](#)] [[PubMed](#)]
7. Yeung, A.T.Y.; Gellatly, S.L.; Hancock, R.E.W. Multifunctional cationic host defence peptides and their clinical applications. *Cell. Mol. Life Sci.* **2011**, *68*, 2161–2176. [[CrossRef](#)] [[PubMed](#)]
8. Madani, F.; Lindberg, S.; Langel, Ü.; Futaki, S.; Gräslund, A. Mechanisms of Cellular Uptake of Cell-Penetrating Peptides. *J. Biophys.* **2011**, *2011*, 1–10. [[CrossRef](#)] [[PubMed](#)]
9. Hsu, C. Structural and DNA-binding studies on the bovine antimicrobial peptide, indolicidin: Evidence for multiple conformations involved in binding to membranes and DNA. *Nucleic Acids Res.* **2005**, *33*, 4053–4064. [[CrossRef](#)] [[PubMed](#)]
10. Gottenbos, B. Antimicrobial effects of positively charged surfaces on adhering Gram-positive and Gram-negative bacteria. *J. Antimicrob. Chemother.* **2001**, *48*, 7–13. [[CrossRef](#)] [[PubMed](#)]
11. Eppard, R.M.; Vogel, H.J. Diversity of antimicrobial peptides and their mechanisms of action. *Biochim. Biophys. Acta Biomembr.* **1999**, *1462*, 11–28. [[CrossRef](#)]
12. Bacalum, M.; Radu, M. Cationic Antimicrobial Peptides Cytotoxicity on Mammalian Cells: An Analysis Using Therapeutic Index Integrative Concept. *Int. J. Pept. Res. Ther.* **2015**, *21*, 47–55. [[CrossRef](#)]
13. Park, A.J.; Okhovat, J.P.; Kim, J. Antimicrobial peptides. In *Clinical and Basic Immunodermatology*, 2nd ed.; Springer: Cham, Switzerland, 2017; pp. 81–95. [[CrossRef](#)]
14. Kreuzer, A.G.; Salvesson, P.J.; Yang, H. Standard Practices for Fmoc-Based Solid-Phase Peptide Synthesis in the Nowick Laboratory. *Retrieved Sept.* **2018**, *19*, 1–14.
15. Amblard, M.; Fehrentz, J.; Martinez, J.; Subra, G. Methods and Protocols of Modern Solid Phase Peptide Synthesis. *Mol. Biotechnol.* **2006**, *33*, 239–254. [[CrossRef](#)]
16. Huber, U.; Majors, R.E. *Principles in Preparative HPLC*; Agilent Technologies Inc.: Santa Clara, CA, USA, 2007.
17. Tapeinou, A.; Matsoukas, M.-T.; Simal, C.; Tselios, T. Review cyclic peptides on a merry-go-round; towards drug design. *Biopolymers* **2015**, *104*, 453–461. [[CrossRef](#)] [[PubMed](#)]
18. Clinical and Laboratory Standards Institute. *M100 Performance Standards for Antimicrobial*; CLSI: Wayne, PA, USA, 2018; ISBN 1562388045.
19. Labute, P. LowModeMD—Implicit Low-Mode Velocity Filtering Applied to Conformational Search of Macrocycles and Protein Loops. *J. Chem. Inf. Model.* **2010**, *50*, 792–800. [[CrossRef](#)] [[PubMed](#)]